Detectability Of Defects In The Presence Of Linear Nuisance Parameters And Images Signal-Dependent Noise

Rémi Cogranne

DETECTABILITY OF DEFECTS IN THE PRESENCE OF LINEAR NUISANCE PARAMETERS AND IMAGES SIGNAL-DEPENDENT NOISE

Rémi Cogranne

Troyes University of Technology (UTT), Troyes, FRANCE

ABSTRACT

This paper addresses two general problems of imaging systems used for visual inspection and defect detection. On the one hand, the inspected object should be carefully removed in order to detect a potential defect or an anomaly. On the other hand, one of the features of imaging systems is that the noise level depends on the image intensity and so does the detectability of defects. In addition, due to the aging of the acquisition system (LEDs, Reflector), the intensity of the illumination decreases gradually over time. The present paper addresses jointly the impact of aging imaging systems and its ensuing impact on the detectability of a defect in the presence of linear nuisance parameters and signal-dependent noise.

***Index Terms*—** Nondestructive testing, Signal-dependent noise, Nuisance parameters, Defects detection.

1. INTRODUCTION

Imaging system for process monitoring and non-destructive are nowadays widespread in the industrial sector for a very wide range of objects such as fabrics [1–3], nuclear fuel rods [4], steel [5–7] or even food [8]. In brief, such a monitoring process rest on two pillars ; on the one hand, an imaging system capture a photograph of products. On the other hand, a model of an acceptable product is given. The system should inspect the image and verify that the product complies with the model provided. For a vast majority of inspected products, this conformity check does not raise an alarm. However, some products do not pass this test and hence are classified as defective. Depending on the specific application a reliability criterion is usually prescribed as a constraint on either false-alarm or missed-detection rates.

The prior methods for detection of defects based on computer vision can be divided into three categories [1, 9]: 1) Several highly flexible techniques do not require a precise prior knowledge of inspected objects and instead rely on usual tools for image processing and defect enhancements such as edge detection, contrast enhancement and pattern recognition, see for instance [2, 10]. 2) Specific methods can be designed using a ground truth or examples of a reference object [9]. Detection methods of this group are usually simple as they are often based on differences between the reference and the inspected image. 3) Methods based on computer vision and image processing see [11, Chap. 15] usually requires prior information on the non-anomalous object. Two main approaches have been proposed to introduce statistical prior knowledge: Bayesian and non-Bayesian approaches. Methods of the first group usually lack precise description of non-anomalous products and hence achieve a limited detection performance. On the opposite, methods based on examples of references are usually simple and accurate but are extremely sensitive to acquisition condition and settings. For a more detailed review on methods for automatic defects detection, the reader is referred to [9, 12].
Regardless of the inspection method, their common underlying goal is to deal with a nuisance parameters that the non-anomalous product is; the defect is to be detected within a possible complex "background" which should be carefully considered. In addition, the detectability of defects always depends on the "defect-to-noise" ratio and one of the specificities of imaging system lies in its well-known signal-dependent noise [13, 14] which is due Poisson noise resulting from the photon-counting process.

Within this context, the present paper studies the impact of the unavoidable aging of imaging system elements on the detectability of defects in the presence of a nuisance parameter (the non-anomalous object "background") and the specific image signal-dependent noise. Using hypothesis testing theory, we model the degradation of detection accuracy of an optimal test for defect detection in the presence of a linear nuisance parameter [15, 16]. The proposed methodology can be applied to almost every non-destructive system that is based on computer vision and for which a minimal level of defect detection accuracy is required. In addition we propose a simple yet efficient method for taking into account the signal-dependent noise characteristics and show that the loss of performance is rather limited.

The present paper is organized as follows. First, Section 2 recalls the heteroscedastic model of noise corrupting images. Then Section 3 presents the main results of our previous work on the application of hypothesis testing to the problem of defect detection in the presence of a linear nuisance parameter [15–19]. Then Section 4 studies the impact of illumination system aging and also presents the method proposed to deal

with signal-dependent noise. Eventually, Section 5 presents numerical results for a real practical case of wheels coating inspection and Section 6 concludes the paper.

2. SIGNAL-DEPENDENT IMAGE NOISE MODEL

Because the present paper focuses on imaging systems based monitoring processes, it is proposed to start modelling the noise of digital cameras. Without loss of generality, let us denote the recorded image $\mathbf{z}$ as a vector of M pixels: $\mathbf{z} = \{z_m\}$, $m \in \{1, \ldots, M\}$. A very popular model for image representation that is widely used in image processing [13–15, 20–23] consists in assuming that an image can be represented as:

$$\mathbf{z} = \boldsymbol{\mu} + \mathbf{N}, \tag{1}$$

where $\boldsymbol{\mu} = \{\mu_m\}$, $m \in \{1, \ldots, M\}$ is the vector representing the expectation of pixels, that is the "theoretical image value", and $\mathbf{N} = \{n_m\}$, $m \in \{1, \ldots, M\}$ denotes the additive.

Most visual inspection system prevents processing the acquired image before its analysis ; therefore we will use the well-established signal-dependent noise model. It comes, on the one hand, from the photon-counting process give birth to a Poisson noise and, on the other hand, from a while Gaussian noise which is caused by various sources (thermal noise, electronic and readout noise, etc.). In addition, on the photosensor, it can be observed that pixels' value are uncorrelated, see [13,14]. Using the Gaussian approximation of the Poisson law for large numbers allows the modelling of pixel values as the following Gaussian random variable:

$$z_m \sim \mathcal{N}(\mu_m, \sigma_m^2), \tag{2}$$

where $\mathcal{N}$ denotes the Gaussian distribution and the variance of pixel z_m is given as an affine function of expectation μ_m as:

$$\sigma_m^2 = a\,\mu_m + b. \tag{3}$$

In Equation (3) the parameters (a, b) of the so-called heteroscedastic noise model remain the same for all the pixels as they only depend on the acquisition parameters (such as the ISO sensitivity, the exposure time and the photosensor) which are constant in a regular monitoring process [13, 14]. Using the same vector representation as in Eq. (1), the heteroscedastic noise model can be represented as:

$$\mathbf{z} \sim \mathcal{N}(\boldsymbol{\mu}, \boldsymbol{\Sigma}), \tag{4}$$

where the diagonal covariance matrix $\boldsymbol{\Sigma}$ is given by $\boldsymbol{\Sigma}_{m,k} = 0$ for all $m \neq k$ and $\boldsymbol{\Sigma}_{m,m} = \sigma_m^2 = a\,\mu_m + b$.

3. DEFECT DETECTION IN THE PRESENCE OF A LINEAR NUISANCE PARAMETER

Though the present paper has been applied in the specific application appearance detection on wheels' surface, see Section 5and our prior works [15, 16], is applied more generally to the broad problem of unknown defect detection in the presence of linear nuisance parameters. This model is often used in hypothesis testing as it offers great flexibility and a good tradeoff between accuracy and simplicity [15–19]. Using this model, the vector of all pixels expectation, for a non-anomalous object, is modelled as

$$\boldsymbol{\mu} = \mathbf{H}\mathbf{d}. \tag{5}$$

The matric $\mathbf{H}$ of size (M, n) represent the non-anomalous "background" over which the potential defect can occur.

Taking into account the heteroscedastic model described in Section 2 the problem of unknown defect detection in the presence of a linear nuisance parameter can be formalized as a choice between the following statistical hypotheses:

$$\begin{cases} \mathcal{H}_0 \;:\; \{\mathbf{z} \sim \mathcal{N}(\mathbf{H}\mathbf{d}, \boldsymbol{\Sigma})\}, \\ \mathcal{H}_1 \;:\; \{\mathbf{z} \sim \mathcal{N}(\mathbf{H}\mathbf{d} + \boldsymbol{\theta}, \boldsymbol{\Sigma}),\, \boldsymbol{\theta} \neq \mathbf{0}\}. \end{cases} \tag{6}$$

In the Equation (6) the unknown vector $\boldsymbol{\theta}$ represents the potential defect it is aimed at detecting.
One can note from the definition of the detection problem (6) several difficulties ; first the non-anomalous "background" $\boldsymbol{\mu} = \mathbf{H}\mathbf{d}$ is a nuisance parameter in the sense that it has no interest for the detection of defect $\boldsymbol{\theta}$ while it must be carefully taken into account. Besides the variance changes for each pixel as, within the signal-dependent noise model (3)-(4), it depends on their expectation which is unknown. Last, on a more practical point of view, because of the aging of the overall imaging system, the illumination decreases gradually. One must thus take into account the impact of this declining brightness on the statistical performance of the defect detection problem (6) especially to maintain the desired requirement on detection accuracy and this is the main scope of the present paper. Surprisingly, to the best of our knowledge, this has never been studied.

The reader interested in the targeted application can read [15, 16], without going much into details those works proposed an original method for designing an auto-adaptive data-driven linear parametric model such as in [18].

Let us start assuming that both the linear model $\mathbf{H}$ and the noise covariance matrix $\boldsymbol{\Sigma}$ are known. In such a case, it has been shown in [26] that two equivalent methods can be used. First one can "normalize" the pixels:

$$\mathbf{z}' = \boldsymbol{\Sigma}^{-1/2}\mathbf{z}. \tag{7}$$

Because the covariance matrix $\boldsymbol{\Sigma}$ is symmetric positive definite, there exists a non-singular symmetric matrix $\boldsymbol{\Sigma}^{1/2}$ such that $\boldsymbol{\Sigma} = \boldsymbol{\Sigma}^{1/2}\boldsymbol{\Sigma}^{1/2}$ and hence $\boldsymbol{\Sigma}^{-1} = \boldsymbol{\Sigma}^{-1/2}\boldsymbol{\Sigma}^{-1/2}$.
It immediately follows from the multivariate Gaussian distribution that the testing problem (6) becomes :

$$\begin{cases} \mathcal{H}_0 : \left\{\mathbf{z}' \sim \mathcal{N}(\boldsymbol{\Sigma}^{-1/2}\mathbf{H}\mathbf{d}, \boldsymbol{I}_M)\right\}, \\ \mathcal{H}_1 : \left\{\mathbf{z}' \sim \mathcal{N}(\boldsymbol{\Sigma}^{-1/2}\mathbf{H}\mathbf{d} + \boldsymbol{\Sigma}^{-1/2}\boldsymbol{\theta}, \boldsymbol{I}_M),\, \boldsymbol{\theta} \neq \mathbf{0}\right\}, \end{cases} \tag{8}$$

where $\mathbf{I}_M$ denotes the identity matrix of size $M \times M$. Then the detection problem (8) can be addressed by leveraging the invariance principle, see [24, Chap. 6] and [25, Chap. 4]. In the present application, it can be used by projecting the "normalized pixels" $\mathbf{z}'$ onto the orthogonal complement of the subspace spanned by the columns of $\mathbf{\Sigma}^{-1/2}\mathbf{H}$, that is its null space. Let

$$\mathbf{P}_{\mathbf{H}}^{\perp} = \mathbf{I}_M - \mathbf{\Sigma}^{-1/2}\mathbf{H}\left(\mathbf{H}^{\mathrm{T}}\mathbf{\Sigma}^{-1}\mathbf{H}\right)^{-1}\mathbf{H}^{\mathrm{T}}\mathbf{\Sigma}^{-1/2}, \quad (9)$$

and let the $\mathbf{W}^{\mathrm{T}} = (w_1, \ldots, w_{M-h})$ be the matrix of size $(M, M-h)$ composed of the eigenvectors $w_1, \ldots, w_{M-h}$ of $\mathbf{P}_{\mathbf{H}}^{\perp}$ corresponding to the eigenvalue 1, it satisfies the following conditions: $\mathbf{W}\mathbf{\Sigma}^{-1/2}\mathbf{H} = \mathbf{0}$ and $\mathbf{W}^{\mathrm{T}}\left(\mathbf{W}\mathbf{W}^{\mathrm{T}}\right)^{-1}\mathbf{W} = \mathbf{P}_{\mathbf{H}}^{\perp}$.

It is shown in [26] that the $\mathbf{W}\mathbf{z}$ is statistics maximal invariant $\mathbf{H}$ and, hence, that all invariant tests should depend on $\mathbf{z}$ only via $\mathbf{W}\mathbf{z}$. In addition, it is shown that a Uniformly Best Constant Power (UBCP) test can be designed based on the norm of the so-called residuals:

$$\Lambda(\mathbf{z}) = \left\|\mathbf{P}_{\mathbf{H}}^{\perp}\mathbf{\Sigma}^{-1/2}\mathbf{z}\right\|_2^2 \quad (10)$$

$$= \mathbf{z}^{\mathrm{T}}\mathbf{\Sigma}^{-1/2}\mathbf{W}^{\mathrm{T}}\left(\mathbf{W}\mathbf{W}^{\mathrm{T}}\right)^{-1}\mathbf{W}\mathbf{\Sigma}^{-1/2}\mathbf{z}. \quad (11)$$

as follows:

$$\delta = \begin{cases} \mathcal{H}_0 & \text{if } \Lambda(\mathbf{z}) < \tau \\ \mathcal{H}_1 & \text{if } \Lambda(\mathbf{z}) \geq \tau, \end{cases} \quad (12)$$

In addition,the properties of the Gaussian distribution yields that the maximal invariant statistics $\Lambda(\mathbf{z})$ follows a (non-central) χ^2. The non-central parameter, denoted ϱ equals 0 under hypothesis $\mathcal{H}_1$ while, on the opposite, it is given, under hypothesis $\mathcal{H}_1$, by :

$$\varrho = \left\|\mathbf{P}_{\mathbf{H}}^{\perp}\mathbf{\Sigma}^{-1/2}\boldsymbol{\theta}\right\|_2^2. \quad (13)$$

Therefore, in order to guarantee the false-alarm probability α_0, the decision threshold τ is set as follows:

$$\tau = F^{-1}_{\chi^2_\Upsilon}(1-\alpha_0; 0), \quad (14)$$

where $F_{\chi^2_\Upsilon}(x, \varrho)$ and $F^{-1}_{\chi^2_\Upsilon}(x, \varrho)$) represent respectively the non-central χ^2 cumulative distribution function and its inverse with non-centrality parameter ϱ and $\Upsilon = M - h$ degree of freedom.
Similarly the power function of the test is given by:

$$\beta(\delta, \boldsymbol{\theta}) = F_{\chi^2_\Upsilon}(\tau, \varrho). \quad (15)$$

3.1. Impact of Illumination Aging on Defect Detection

Let us first emphasize that it follows from Eq. (14)-(15) that the detectability of the defect is entirely characterized by the "anomaly-to-noise" ratio (13). Therefore, it is sufficient to investigate the evolution of the non-centrality parameter ϱ in order to study the crucial effect that the illumination system (or the light intensity) has on the accuracy of defect detection. To this end, we will consider that the intensity in multiply by a factor γ : $\boldsymbol{\mu}_2 = \gamma\boldsymbol{\mu}_1$ (1)-(5) where $\gamma \in]0, 1[$ represents the impact of the system again on the illumination. Reminding that under the signal-dependent noise model corrupting raw images, used for the visual inspection system, it follows from the signal-dependent noise model (3)-(4) that $\mathbf{\Sigma}_1 = \mathrm{diag}(a\boldsymbol{\mu}_1 + b)$ and $\mathbf{\Sigma}_2 = \mathrm{diag}(a\boldsymbol{\mu}_2 + b) = \mathrm{diag}(a\gamma\boldsymbol{\mu}_1 + b)$. Here diag is the vector representing the (non-zero) elements of diagonal matrices.

We will investigate the effect of illumination again by comparing ϱ_1 and ϱ_2 (13). It follows that:

$$\varrho_2 = \left\|\mathbf{P}_{\mathbf{H}}^{\perp}{\mathbf{\Sigma}_2}^{-1/2}\gamma\boldsymbol{\theta}\right\|_2^2 = \gamma^2\left\|\mathbf{P}_{\mathbf{H}}^{\perp}{\mathbf{\Sigma}_2}^{-1/2}\boldsymbol{\theta}\right\|_2^2. \quad (16)$$

Because pixels are independent the covariance matrices are diagonal and hence:

$$\varrho_1 = \sum_{m=1}^{M}\frac{\left(\mathbf{P}_{\mathbf{H}}^{\perp}\boldsymbol{\theta}\right)_m^2}{a\boldsymbol{\mu}_m + b}, \quad (17)$$

and similarly

$$\varrho_2 = \gamma^2\sum_{m=1}^{M}\frac{\left(\mathbf{P}_{\mathbf{H}}^{\perp}\boldsymbol{\theta}\right)_m^2}{a\gamma\boldsymbol{\mu}_m + b}. \quad (18)$$

Let us now study is the decrease of illumination decreases the non-centrality parameter and hence the detection accuracy:

$$\varrho_2 < \varrho_1 \;\Leftrightarrow\; \gamma^2\sum_{m=1}^{M}\frac{\left(\mathbf{P}_{\mathbf{H}}^{\perp}\boldsymbol{\theta}\right)_m}{a\gamma\boldsymbol{\mu}_m + b} < \sum_{m=1}^{M}\frac{\left(\mathbf{P}_{\mathbf{H}}^{\perp}\boldsymbol{\theta}\right)_m}{a\boldsymbol{\mu}_m + b}, \quad (19)$$

$$\Leftrightarrow \sum_{m=1}^{M}\left(\mathbf{P}_{\mathbf{H}}^{\perp}\boldsymbol{\theta}\right)_m^2\left(\frac{\gamma^2}{a\gamma\boldsymbol{\mu}_m + b} - \frac{1}{a\boldsymbol{\mu}_m + b}\right) < 0. \quad (20)$$

Because the first part of Eq. (20) is positive the inequality holds true if the second part is negative which immediately yields:

$$\gamma^2(a\boldsymbol{\mu}_m + b) - \gamma(a\boldsymbol{\mu}_m) - b < 0. \quad (21)$$

Solving the quadratic Eq. (21) immediately shows that:

$$\varrho_2 < \varrho_1 \Leftrightarrow \begin{cases} 0 < \gamma < 1 & \text{if } b \geq 0 \\ \frac{-b}{a\boldsymbol{\mu}_m + b} < \gamma < 1 & \text{if} b < 0 \text{and} \boldsymbol{\mu}_m > -\frac{2b}{a} \end{cases} \quad (22)$$

For a vast majority of the sensor, the parameter $b > 0$ and the first case (22) applies. This confirms that when the illumination decreases, so does the detectability of a potential defect. Note that there are some sensors for which $b < 0$ because of a pedestal parameter which is added to pixel value. However, even in this case, the value of parameter a and b which ensures that pixels expectation μ always satisfies $\mu > \frac{-2b}{a}$ in

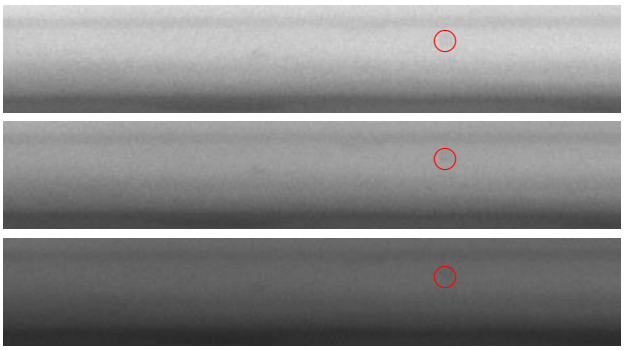

Fig. 1. Examples of the impact of the wheels illumination intensity on the detectability of the very same defect.

practice.
This impact of illumination aging is pictured in the Figure 1. It especially helps visualize that a decrease in the illumination degrades the detectability by (1) reducing the strength of the defect itself and (2) degrading the "defect-to-noise ratio" ϱ due to the signal-dependent noise of images.

4. PROPOSED METHODOLOGY FOR DEALING WITH SYSTEM ILLUMINATION AGING

In practice the approach defined in the Section 3 is hardly applicable because the expectation of pixels is unknown (mostly because the nuisance parameter $\mathbf{Hd}$ is unknown) and so does is the covariance matrix $\mathbf{\Sigma}$ under the signal-dependent noise model (3)-(4). To deal with this problem, we propose a two steps approach. First, a coarse estimation of pixel expectation is made without taking into account the variation of variance using a simple ordinary Least-Square (LS):

$$\begin{cases} \widetilde{\boldsymbol{\mu}}_{\text{ls}} = \mathbf{H}\left(\mathbf{H}^{\text{T}}\mathbf{H}\right)^{-1}\mathbf{H}^{\text{T}}\mathbf{z}, \\ \widetilde{\mathbf{\Sigma}}_{\text{ls}} = \mathbf{I}_M \times (a\,\widetilde{\boldsymbol{\mu}}_{\text{ls}} + b), \end{cases} \tag{23}$$

Secondly, this rough estimation of the covariance is reused to update the estimation of the expectation using the well-known Weighted Least-Square (WLS) given by:

$$\begin{cases} \widetilde{\boldsymbol{\mu}} = \widetilde{\mathbf{\Sigma}}_{\text{ls}}^{-1/2}\mathbf{H}\left(\mathbf{H}^{\text{T}}\widetilde{\mathbf{\Sigma}}_{\text{ls}}^{-1}\mathbf{H}\right)^{-1}\mathbf{H}^{\text{T}}\widetilde{\mathbf{\Sigma}}_{\text{ls}}^{-1/2}\mathbf{z}, \\ \widetilde{\mathbf{\Sigma}} = \mathbf{I}_M \times (a\,\widetilde{\boldsymbol{\mu}} + b). \end{cases} \tag{24}$$

Here, $\widetilde{\boldsymbol{\mu}}$ represents the non-anomalous background of pixels from $\mathbf{z}$. Finally, the statistical test (12) is applied using the estimations of pixels expectation and variance as given in (24):

$$\delta = \begin{cases} \mathcal{H}_0 & \text{if } \widetilde{\Lambda}(\mathbf{z}) < \tau \\ \mathcal{H}_1 & \text{if } \widetilde{\Lambda}(\mathbf{z}) \geq \tau, \end{cases} \tag{25}$$

with the test statistics :

$$\widetilde{\Lambda}(\mathbf{z}) = \left\| \widetilde{\mathbf{P}}_{\mathbf{H}}^{\perp}\widetilde{\mathbf{\Sigma}}^{-1/2}\mathbf{z} \right\|_2^2 \tag{26}$$

$$\text{and } \widetilde{\mathbf{P}}_{\mathbf{H}}^{\perp} = \mathbf{I}_M - \widetilde{\mathbf{\Sigma}}^{-1/2}\mathbf{H}\left(\mathbf{H}^{\text{T}}\widetilde{\mathbf{\Sigma}}^{-1}\mathbf{H}\right)^{-1}\mathbf{H}^{\text{T}}\widetilde{\mathbf{\Sigma}}^{-1/2}. \tag{27}$$

4.1. Impact of Linear Nuisance Parameter Estimation

Last but not least, it is important to measure the effect of using an estimation of both pixels expectation and variance on the statistical performance of the test (25). To this end, let us recall that using the proposed linear model for nuisance parameter (5) as well as the signal-dependent noise of raw images (3) the pixels follow a multivariate Gaussian distribution $\mathbf{z} \sim \mathcal{N}(\mathbf{Hd}, \mathbf{\Sigma})$ with $\mathbf{\Sigma} = \text{diag}\left(\sigma_1^2, \ldots, \sigma_M^2\right)$.
When the covariance matrix $\mathbf{\Sigma}$ is unknown, it immediately follows from the properties of multivariate Gaussian distribution that:

$$\widetilde{\mathbf{P}}_{\mathbf{H}}^{\perp}\widetilde{\mathbf{\Sigma}}^{-\frac{1}{2}}\mathbf{z} \sim \mathcal{N}\left(\widetilde{\mathbf{P}}_{\mathbf{H}}^{\perp}\widetilde{\mathbf{\Sigma}}^{-\frac{1}{2}}\mathbf{Hd}, \widetilde{\mathbf{P}}_{\mathbf{H}}^{\perp\,\text{T}}\widetilde{\mathbf{\Sigma}}^{-\frac{1}{2}^{\text{T}}}\mathbf{\Sigma}\widetilde{\mathbf{\Sigma}}^{-\frac{1}{2}}\widetilde{\mathbf{P}}_{\mathbf{H}}^{\perp}\right) \tag{28}$$

Regarding the expectation is it straightforward that:

$$\begin{aligned} &\widetilde{\mathbf{P}}_{\mathbf{H}}^{\perp}\widetilde{\mathbf{\Sigma}}^{-1/2}\mathbf{Hd} \\ &\quad = \widetilde{\mathbf{\Sigma}}^{-1/2}\mathbf{Hd} - \widetilde{\mathbf{\Sigma}}^{-1/2}\mathbf{H}\underbrace{\left(\mathbf{H}^{\text{T}}\widetilde{\mathbf{\Sigma}}^{-1}\mathbf{H}\right)^{-1}\mathbf{H}^{\text{T}}\widetilde{\mathbf{\Sigma}}^{-1}\mathbf{H}}_{=\mathbf{I}_h}\mathbf{d} \\ &\quad = \widetilde{\mathbf{\Sigma}}^{-1/2}\mathbf{Hd} - \widetilde{\mathbf{\Sigma}}^{-1/2}\mathbf{Hd} = \mathbf{0}. \end{aligned}$$

From which one eventually has

$$\widetilde{\mathbf{P}}_{\mathbf{H}}^{\perp}\widetilde{\mathbf{\Sigma}}^{-1/2}\mathbf{z} \sim \mathcal{N}\left(\mathbf{0}, \widetilde{\mathbf{P}}_{\mathbf{H}}^{\perp\,\text{T}}\widetilde{\mathbf{\Sigma}}^{-1/2^{\text{T}}}\mathbf{\Sigma}\widetilde{\mathbf{\Sigma}}^{-1/2}\widetilde{\mathbf{P}}_{\mathbf{H}}^{\perp}\right) \tag{29}$$

This shows that the estimation of pixels' expectation is unbiased and, therefore, so does is the estimation of pixels' variances.
The only source of loss of detection performance due to the estimation and rejection of nuisance parameters is due to the variance of the estimation of the covariance matrix.

5. EXPERIMENTS AND RESULTS

The application targeted in the present paper is the control of wheels during its manufacturing process and especially the detection of coating defects. The image 2 shows a typical example of an image used to carry out the coating inspection and the defect detection. This image shows, on the one hand, the different parts of the wheels (in white) and, on the other hand, the feature elements (in red). The latter are used to split the locate the different parts. Thanks to this localization of the feature elements, the image can be split in order to inspect each part separately after being transformed into a rectangle

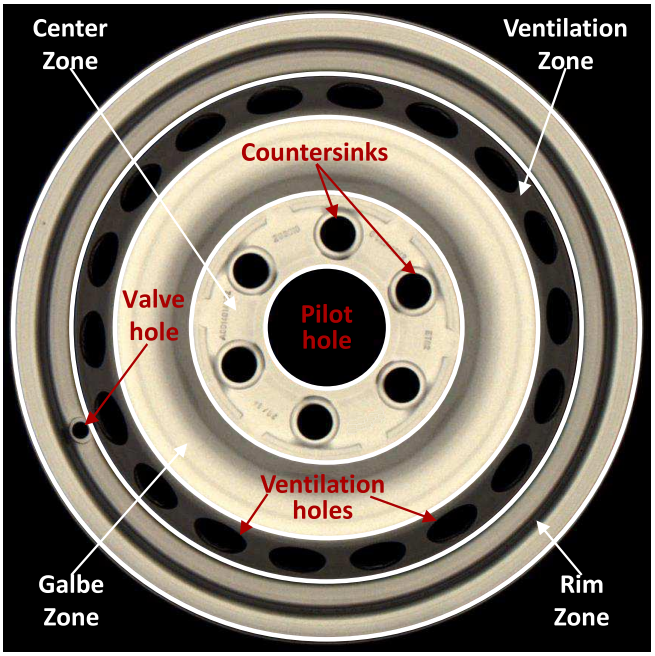

Fig. 2. An example of an image wheel obtained with our imaging system along with the description of main parts.

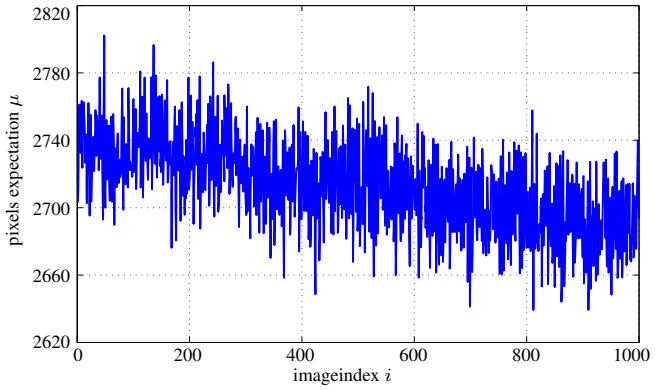

Fig. 3. An example of a real evolution of the mean value of pixels showing the illumination system aging impact of brightness.

to help the inspection. An illustrative result of such a transformation of the galbe zone in illustrated in Figure 1. The reader is referred to [15, 16] for more detail on the linear model of pixels' expectation $\boldsymbol{\mu} = \mathbf{Hd}$ as in Eq. (5).

Nevertheless, the present problem is more general and applies to all monitoring process based on a computer vision in which light source and reflector are undoubtedly subject to aging [27].The Figure 3 presents a typical example of decrease in the average pixels' values resulting from again of artificial light sources and deposit of dust on light reflector surface.

This issue is important since as shown in Sections 3-4 the detectability highly depends on the acquired image brightness. For an industrial application of such a computer vision system for monitoring, one should warrant a certain level of defect detection accuracy and hence signal when the illumination is not sufficient anymore. Our methodology consists in using a minimal defect $\boldsymbol{\theta}_{\min}$ for which the illumination complies with a "defect-to-noise" ratio ϱ (13) that allows maintaining a minimal detection power $\beta_{\min}$ (15) under a false-alarm constraint (14).

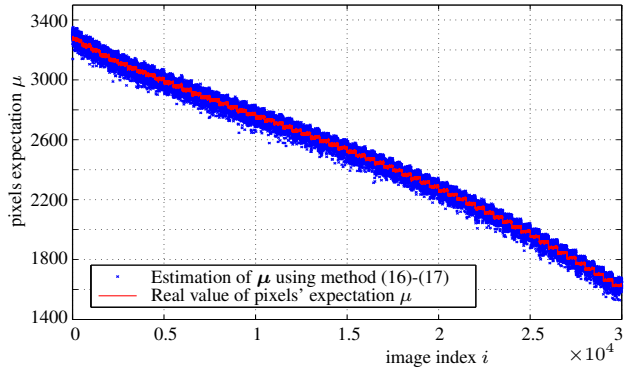

Fig. 4. Simulated of the mean value of pixels illustrating the illumination system aging impact of brightness.

To verify the sharpness and the relevance of the proposed method we have simulated illumination system again at an accelerated pace (simply by decreasing light intensity regularly). The Figure 4 show the accelerated evolution of the illumination via the average value of all pixels from wheel images. Contrast the real value (in red) with the estimation obtained using the method described in Eq. (23)-(24).

Figure 5 presents the empirical and theoretical distributions of the proposed test statistics $\widetilde{\Lambda}(\mathbf{z})$, see Eq [**?**]. Those results were obtained with real data using the following experimental protocol: a single wheel with the defect was placed in the imaging device of visual inspection system. The conveyor was halted and many images were captured successively without modifying the illumination. We extracted a small area of 20×20 pixels over which the defect $\boldsymbol{\theta}$ is present. We have measured that for this illumination, for which pixels mean value was about $\mu = 3400$ the defect detectability was about $\varrho \approx 340$, see Eq. (13).

As it can be seen in Figure 5 the theoretical and the empirical distributions match almost perfectly. Note the shift in the expectation of the distribution that corresponds to the defect testability (the χ^2 distribution non-centrality parameter). Interestingly, one can note the very small increase of variance (especially under $\mathcal{H}_1$) that is due to the use of the estimation of variance obtained using estimated pixels expected values as described in Eq. (23)-(24).

Last, Figure 6 compares the empirical and theoretical detection power functions. Again, those results have been obtained on real wheels image using the same protocol except that now the power of LEDs was reduced every 500 images.

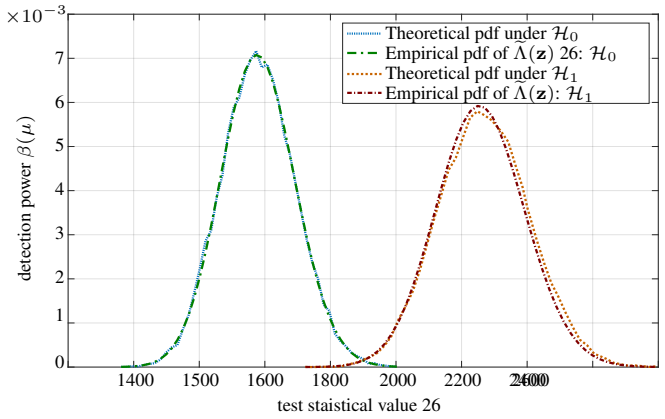

Fig. 5. Statistical distribution of the proposed test statistics $\widetilde{\Lambda}(\mathbf{z})$ 26: comparison between empirical observation and theoretical distribution.

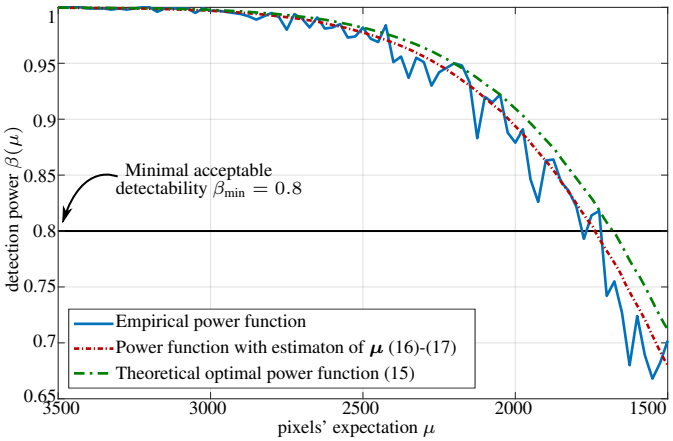

Fig. 6. Evolution of detection performance as a function of the decreasing illumination (pixels expectation).

For the sake of the presentation, we assumed that the defect corresponds to the minimal one that it is wished to detect $\boldsymbol{\theta}_{\min}$. Note this experimental setup was used to obtain data for Figure 1. In our present case, the minimal detection accuracy is $\beta_{\min} = 0.8$ and the false alarm rate is $\alpha_0 = 0.02$.
We calculated the theoretical detection power β (15) when the variance of pixels is known and when it is estimated as in Eq. (23)-(24). The empirical detection power matches very well the theoretical findings. Note that the empirical data is very noisy because we used "only" 500 images for every brightness level while using a low false alarm rate $\alpha_0 = 0.02$. Here again the theoretically established power match almost perfect with the one theoretically established. Note that in order computed the power function when the pixel expectation is to know we simply averaged pixel values over the 500 images with the same illumination: this provides a practical rather very accurate upper bound (shown in green) that can be used practically using a simple photometer in the visual inspection system.

6. CONCLUSION

This paper shows how the signal-depend noise model of image impact defects detectability and focuses on the impact of decreasing illumination due to the aging of the illumination system. We propose a simple yet efficient method for dealing with the signal dependent noise it limited impact on the detection accuracy. While the paper focuses on the application of wheels inspection, it addresses a general problem for monitoring defect detectability and proposes a practical for which numerical results show the high accuracy and relevance. A future work will study how to use several images as well as the optimal detection when the light intensity reaches the limit defined according to the prescribed detection performance.

7. REFERENCES

[1] A. Kumar, "Computer-vision-based fabric defect detection: a survey," *IEEE Trans. on Industrial Electronics*, vol. 55, no. 1, pp. 348–363, 2008.

[2] R. Stojanovic, *& al.*, "Real-time vision-based system for textile fabric inspection," *Real-Time Imaging*, vol. 7, no. 6, pp. 507–518, 2001.

[3] Y. Zhang, *& al.*, "Fabric defect detection and classification using gabor filters and gaussian mixture model," *Computer Vision–ACCV 2009*, pp. 635–644, 2010.

[4] R. Cogranne and F. Retraint, "Detection of defects in radiographic images using an adaptive parametric model," *Signal Processing*, vol. 96, Part B, pp. 173–189, 2014.

[5] N. Neogi, *& al.*, "Review of vision-based steel surface inspection systems," *EURASIP Journal on Image and Video Processing*, vol. 2014, no. 1, pp. 50, 2014.

[6] W.B. Li, *& al.*, "A local annular contrast based real-time inspection algorithm for steel bar surface defects," *Applied Surface Science*, vol. 258, no. 16, pp. 6080–6086, 2012.

[7] D. Naso, *& al.*, "A fuzzy-logic based optical sensor for online weld defect-detection," *IEEE Trans. on Industrial Informatics*, vol. 1, no. 4, pp. 259–273, 2005.

[8] T. Brosnan and D.W. Sun, "Improving quality inspection of food products by computer vision—-a review," *Journal of Food Engineering*, vol. 61, no. 1, pp. 3–16, 2004.

[9] D. Mery, *& al.*, "A review of methods for automated recognition of casting defects," *J. Brit. Inst. Non-Destructive Testing*, vol. 44, no. 7, pp. 428–436, 2002.

[10] J.B. Martens, "Adaptive contrast enhancement through residue-image processing," *Signal Processing*, vol. 44, no. 1, pp. 1–18, 1995.

[11] H.H Barrett and K. J Myers, *Foundations of image science*, John Wiley & Sons, 2013.

[12] C.H. Chen *& al.*, *Handbook of pattern recognition and computer vision*, vol. 27, World Scientific, 2010.

[13] A. Foi *& al.*, "Practical poissonian-gaussian noise modelling and fitting for single-image raw-data," *IEEE Trans. on Image Processing*, vol. 17, no. 10, pp. 1737–1754, 2008.

[14] T.H. Thai, *& al.*, "Statistical Model of Quantized DCT Coefficients: Application in the Steganalysis of Jsteg Algorithm," *IEEE Trans. on Image Processing*, vol. 23, no. 5, pp. 1980-1993, 2014.

[15] K. Tout,, *& al.*, "Fully automatic detection of anomalies on wheels surface using an adaptive accurate model and hypothesis testing theory," in *Signal Processing Conference (EUSIPCO),*. IEEE, 2016, pp. 508–512.

[16] K. Tout, *& al.*, "Fully automatic detection of anomalies using an adaptive statistical model and testing theory: Application to wheel surface inspection," *Signal Processing*, vol. 144, pp. 430–443, 2018.

[17] T. Nguyen, *& al.*, "Reliable detection of interest flooding attack in real deployment of named data networking," *IEEE Trans. on Information Forensics and Security*, vol. 14, no. 9, pp. 2470–2485, 2019.

[18] R. Cogranne, *& al.*, "Detecting botclouds at large scale: A decentralized and robust detection method for multi-tenant virtualized environments," *IEEE Trans. on Network and Service Management*, vol. 15, no. 1, pp. 68–82, 2018.

[19] I.V. Nikiforov, *& al.*, "Sequential detection of a total instantaneous blockage occurred in a single subassembly of a sodium-cooled fast reactor," *Nuclear Engineering and Design*, vol. 366, pp. 110733, 2020.

[20] V. Sedighi, *& al.*, "Content-adaptive steganography by minimizing statistical detectability," *IEEE Trans. on Information Forensics and Security*, vol. 11, no. 2, pp. 221–234, 2016.

[21] R. Cogranne, *& al.*, "Efficient steganography in jpeg images by minimizing performance of optimal detector," *IEEE Trans. on Information Forensics and Security*, vol. 17, pp. 1328–1343, 2022.

[22] Q. Giboulot, *& al.*, "Multivariate side-informed gaussian embedding minimizing statistical detectability," *IEEE Trans. on Information Forensics and Security*, vol. 17, pp. 1841–1854, 2022.

[23] Q. Giboulot, *& al.*, "Detectability-based jpeg steganography modelling the processing pipeline: The noise-content trade-off," *IEEE Trans. on Information Forensics and Security*, vol. 16, pp. 2202–2217, 2021.

[24] E. L. Lehmann, *Testing statistical hypotheses*, Springer, 1986.

[25] T.S. Ferguson, *Mathematical Statistics: A Decision Theoretic Approach*, Academic Press, 1967.

[26] M. Fouladirad, *& al.*, "Optimal fault detection with nuisance parameters and a general covariance matrix," *Int. J. Adapt. Control Signal Process.*, vol. 22, no. 5, pp. 431–439, 2008.

[27] N. Narendran and Y. Gu, "Life of LED-based white light sources," *Journal of display technology*, vol. 1, no. 1, pp. 167–171, 2005.